Available online at www.sciencedirect.com

ScienceDirect

Procedia Structural Integrity 2 (2016) 112–119

Structural Integrity Procedia

www.elsevier.com/locate/procedia

21st European Conference on Fracture, ECF21, 20-24 June 2016, Catania, Italy

Feasibility study of adhesive bonding reinforcement by electrospun nanofibers

F. Musiari[1]*, A. Pirondi[1], F. Moroni[1], G. Giuliese[2], J. Belcari[2], A. Zucchelli[2], T. M. Brugo[2], G. Minak[2], C. Ragazzini[2]

[1]*Dipartimento di Ingegneria Industriale, Università di Parma*
Parco Area delle Scienze 181/A, 43124 Parma, Italy
web page: http://www.unipr.it

[2]*Dipartimento di Ingegneria Industriale, Alma Mater Studiorum - Università di Bologna*
viale del Risorgimento 2, 40136 Bologna, Italy
web page: http://www.unibo.it

Abstract

In previous works, the authors showed that the interleaving of an electrospun nylon nanofibrous mat at the interface between adjacent plies of a composite laminate increases the delamination strength. In particular, the nanomat acts a net-like reinforcing web, enabling a ply-to-ply bridging effect. This reinforcing property of the nanomats can be potentially used in other applications which need to improve the fracture resistance of interfaces, such as adhesive bonding. The present work analyses the feasibility of an electrospun polymeric nanomat as adhesive carrier and reinforcing web in industrial bonding. Thus the adhesive is used to pre-impregnate a nylon nanofibrous mat that is then placed at the interface between two metal pieces and then cured. The aim of the work is first to assess the effectiveness of this procedure, by comparison of the mode-I fracture toughness measured with DCB (Double Cantilever Beam) tests with and without the reinforcement in the adhesive layer. For this purpose, a 2024-T3 aluminum alloy will be bonded using a general purpose, one-part epoxy resin with low viscosity.

Peer-review under responsibility of the Scientific Committee of PCF 2016.

Keywords: electrospun nanofiber mats, bonding reinforcement, Mode I fracture toughness, adhesive carrier

* Corresponding author. Tel.: +393331296018
E-mail address: francesco.musiari@studenti.unipr.it

Peer review under responsibility of the Scientific Committee of PCF 2016.
10.1016/j.prostr.2016.06.015

1. Introduction

Adhesive bonding is increasingly used in joining structural materials in aerospace, shipments, automotive, wind turbines and other applications as this process facilitates the fabrication of multi-material, light weight structures having high strength to weight ratios (da Silva et al., 2011). Structural adhesives are typically based on Epoxy resins because of the high modulus and strength, low creep and good performance at elevated temperatures. However, epoxy resins are relatively brittle with respect to crack initiation and propagation. Toughening can be obtained, for instance, by addition of organic (rubber-like) or inorganic (mineral, ceramic) particles. However, particles have to be carefully mixed within the adhesive in order to avoid aggregations that may induce stress concentration. The increase of strength and fracture toughness can also be achieved by addition of fibers, either cut or continuous, in the form of a mat that may also act as a carrier for the pre-cured adhesive (see for example Cytec FM or Henkel EA adhesive series), besides being a layer thickness spacer for the bondline.

Ultra-thin nanofibers from a wide variety of materials including polymers, composites, and ceramics may significantly increase the interaction between the fibers and the matrix materials, leading to better reinforcement than conventional fibers (Huang et al., 2003).

Electrospinning provides a simple and versatile method for generating nanofibers. During the last decade more than twenty papers have been devoted to the study of composite laminates modified by integrating electrospun nanofibrous (see Zucchelli et al., 2011). Only a few papers are found instead on the use as reinforcement for adhesive layers (Oh et al. 2014).

In previous works (Palazzetti et al., 2013; Giuliese et al., 2013; Musiari et al., 2015) the authors showed that the interleaving of an electrospun nylon nanofibrous mat at the interface between adjacent plies of a composite laminate increases the delamination strength. In particular, the nanomat acts a net-like reinforcing web, enabling a ply-to-ply bridging effect. This reinforcing property of the nanomats can be potentially used in other applications which need to improve the fracture resistance of interfaces , such as adhesive bonding.

The present work analyses the feasibility a electrospun polymeric nanomat as adhesive carrier and reinforcing web in industrial bonding. Thus the adhesive is used to pre-impregnate a nylon nanofibrous mat that is then placed at the interface between two metal pieces and then cured. The aim of the work is first to assess the effectiveness of this procedure, by comparison of the mode-I fracture toughness measured with DCB (Double Cantilever Beam) tests with and without the reinforcement in the adhesive layer. For this purpose, a 2024-T3 aluminum alloy will be bonded using a general purpose, one-part epoxy resin with low viscosity.

Nomenclature

a	crack length
b	width of the specimen
E	Young's modulus of the adherent
E_a	Young's modulus of the adhesive
G	Mode I strain energy release ratio
G_C	critical value of G at which the damage initiation occurs
G_{SS}	steady-state value of G at which the damage propagates in an approximately stable way
h	thickness of the adherent
I	inertia moment of the adherent
t	thickness of the bonding interface
λ_σ	parameter for the correction of the G formulation according to Krenk model
ν_a	Poisson's coefficient of the adhesive

2. Materials and preparation

The manufacturing of the specimens for the experimental campaign is described in this paragraph.

2.1. Polymeric nanofibrous mats

Nylon 6,6 nanofibrous mats were manufactured by means of an electrospinning procedure. The polymeric solution, mixed with some solvents, was injected in a capillary tube and then in a needle kept in tension by a highly voltage power supply. Therefore, the polymeric solution was subjected to an electric field which induced an electric charge on the solution surface. When the electric field reached a threshold, the repulsive electric forces became bigger than the surface tensions, thus the solution was ejected from the needle and was whipped during the path between the needle and a grounded collecting plate, in which the charged jet was divided by the repulsive electric field into a multitude of nanometric fibers, stacking on each other to form a mat whose thickness could vary from some nanometers to some micrometers. In the current case, the thickness of the nanomat is included in the range between 70 and 90 μm, while the nanofibers have a diameter of 150±20 nm.

2.2. Specimen fabrication

A 2024-T3 aluminum panel was cut and worked in order to obtain some 300x25x15 adherents. The side of them which was aimed to be bonded was then sanded and the surface was appropriately cleaned. Two specimen configurations were considered: the so called 'virgin' configuration and a nanomodified configuration, in which a Nylon 6,6 electrospun nanofiber mat was interleaved between the adherents. The aluminum alloys were bonded together using an epoxy thermosetting impregnation resin used for manufacturing of woven pre-pregs with carbon fiber (kindly provided by Reglass). In order to realize the nanomodified specimens, the nanomat was completely impregnated by the resin on both sides before having been placed in the interface. The low viscosity of the chosen adhesive encouraged the complete flow of the resin through the thickness of the interface fully occupied by the nanomat. In both virgin and the nanomodified joints, a thickness of 60 μm in the interface was gained using some metal sheet placed at both the extremities of the specimen in order to make the thickness of the adhesive in the virgin ones as uniform as possible with respect the other configuration, in which however the metal sheets were placed to make the nanomat occupy the whole thickness even if it had been squeezed during the curing process. An initial 40 mm long crack was given on an extremity of the specimen by the insertion of a polyester sheet. The specimens were placed in a bonding template, which was then inserted in a vacuum bag. This one underwent a 3 hour curing cycle in autoclave, at a temperature of 100°C and a pressure of 6 bar. The vacuum was kept during the curing cycle, in order to increase the ejection of the air trapped within the polymer. The air ejection was further encouraged by the aforementioned low viscosity of the resin. Two virgin specimens and two nanomodified specimens were realized.

3. DCB tests

3.1. Testing methodology

Double Cantilever Beam (DCB) tests were performed according to the international standard ASTM D3433, in displacement control at constant crosshead ratio (0.03 mm/s in the loading phase and of 0.01 mm/s in the unloading phase) in a servo-hydraulic testing machine MTS 810 with a load cell whose maximum allowable load is equal to 3 kN. The entity of the Crack Opening Displacement (COD) was evaluated by an omega clip gage. In order to gain an initial crack with a not artificially created sharp tip, a fatigue pre-cracking phase was performed, until the crack propagated for 5 mm. The DCB test was then executed by the imposition of a load-unload law in rate displacement control: the unloading phase is necessary to gain a reload section of the curve with constant slope, which allows to evaluate the specimen compliance and therefore the actual crack length during the declining part of the force-displacement curve. Fig. 1 shows N01 virgin specimen being tested.

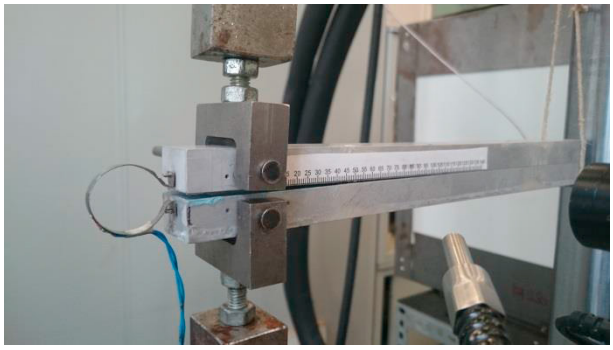

Fig. 1 - DCB test of N01 virgin specimen

3.2. Results and discussion

Firstly, the results relative to the virgin specimens are presented. Fig. 2 presents a force vs. displacement curve relative to the V01 virgin specimen. The numbers identify the force peaks in correspondence of which the compliance is used to evaluate the crack length.

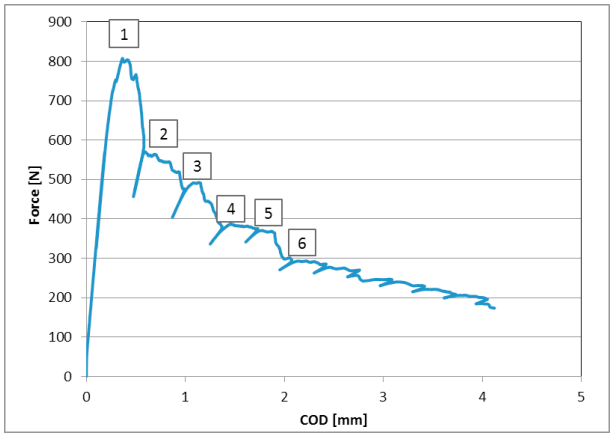

Fig. 2 - Force vs. Crack Opening Displacement (V01 virgin specimen)

Once that the crack length is known, Mode I fracture toughness for each force peak is calculated through the Krenk model (Krenk, 1992), Eq. 1.

$$G = \frac{P^2 a^2}{bEI}\left(1+\frac{1}{\lambda_\sigma a}\right)^2 \tag{1}$$

λ_σ is given by the following expression, Eq. 2.

$$\lambda_\sigma = \sqrt[4]{\frac{6}{h^3 t}\frac{E_a}{E\left(1-\nu_a^2\right)}} \tag{2}$$

Tab. 1 summarizes the values of crack length, load and fracture toughness (evaluated with Eq. 1) in each force peak for the same specimen.

Tab. 1 - Crack length, load and fracture toughness evaluated in each force peak of the V01 virgin specimen

Force peak	Crack length [mm]	Load [N]	Fracture toughness [N/mm]
1	48.91	807.55	0.151
2	70.36	570.69	0.143
3	98.73	492.68	0.198
4	120.44	387.34	0.177
5	129.42	370.50	0.186
6	165.62	292.00	0.184

Fig. 3 and Tab. 2 presents the same results relative to the second virgin specimen (V02).

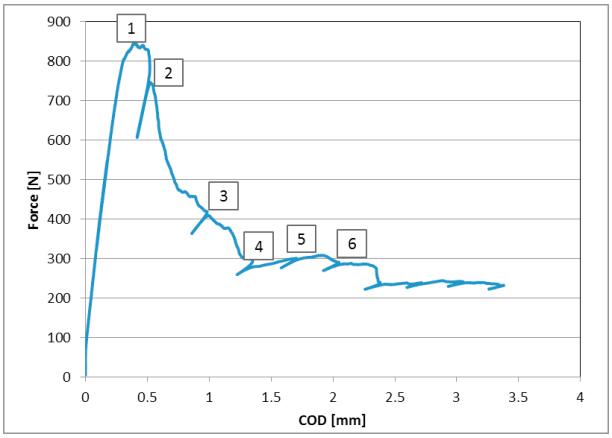

Fig.3 - Force vs Crack Opening Displacement (V02 virgin specimen)

Tab. 2 - Crack length, load and fracture toughness evaluated in each force peak of V02 virgin specimen

Force peak	Crack length [mm]	Load [N]	Fracture toughness [N/mm]
1	51.35	847.77	0.181
2	63.79	746.74	0.206
3	111.80	409.14	0.172
4	151.06	300.90	0.164
5	154.65	307.90	0.180
6	188.90	285.50	0.226

The average values of fracture toughness for the two virgin specimens are 0.173 and 0.188, respectively.

The two nanomodified specimens does not exhibit the same trend of Mode I fracture toughness with respect to the virgin specimens one. In particular, the results relative to the N01 nanomodified specimen are displayed in Fig. 4 and Tab. 3.

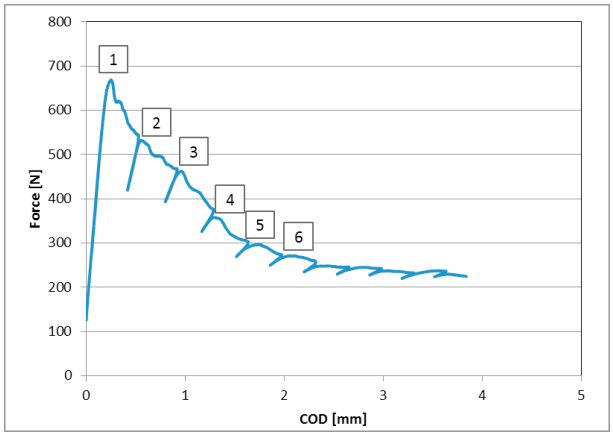

Fig. 4 - Force vs Crack Opening Displacement (N01 nanomodified specimen)

Tab. 3 - Crack length, load and fracture toughness evaluated in each force peak of N01 nanomodified specimen

Force peak	Crack length [mm]	Load [N]	Fracture toughness [N/mm]
1	48.90	669.42	0.104
2	76.31	532.53	0.144
3	95.42	462.51	0.164
4	121.38	345.52	0.143
5	141.52	295.00	0.139
6	164.99	270.70	0.157

The same data referred to the N02 nanomodified specimen are visible in Fig. 5 and Tab. 4.

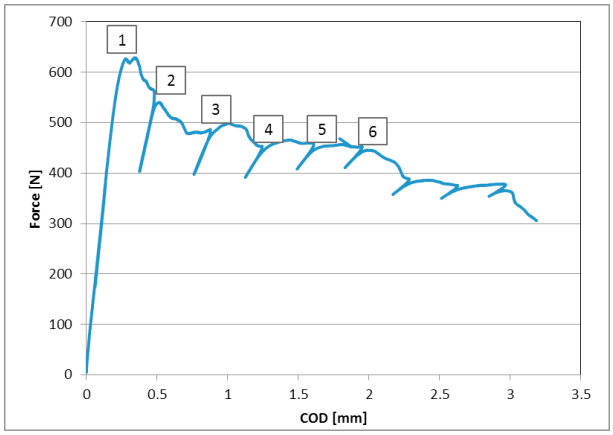

Fig. 5 - Force vs Crack Opening Displacement (N02 nanomodified specimen)

Tab. 4 - Crack length, load and fracture toughness evaluated in each force peak of N02 nanomodified specimen

Force peak	Crack length [mm]	Load [N]	Fracture toughness [N/mm]
1	51.85	625.60	0.100
2	68.59	539.80	0.122
3	88.13	499.40	0.165
4	103.83	465.40	0.194
5	115.62	456.30	0.228
6	124.10	446.50	0.249

An examination of the fracture surface of both the nanomodified specimens reveals that a cohesive breakage of the nanomat occurs, leaving an extremely thin alloy of nanofiber on one adherent and a more relevant and thick portion of it on the other, Fig. 6.

Fig. 6 - Portion of the fracture surface of the N01 nanomodified specimen

The average values of fracture toughness for the two nanomodified specimens are 0.142 and 0.176, respectively. Despite the fact that both the average values are lower than the ones belonging to the virgin specimens, it is possible to notice how the trends of the two nanomodified specimens does not match one another, excepted when the crack length is still small. In particular, it is useful to plot the trend of the Mode I fracture toughness with respect to the crack length for each of the tested specimens, Fig. 7.

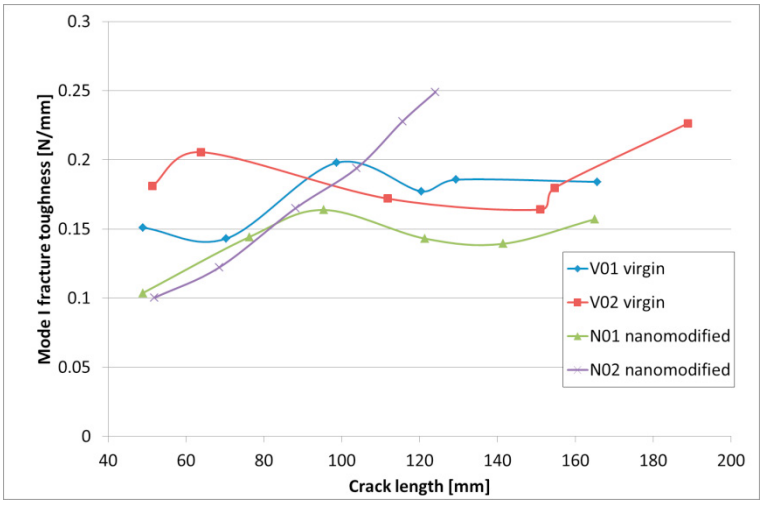

Fig. 7 - Mode I fracture toughness vs crack length

By the observation of the curves, it is possible to state that, while the N01 nanomodified specimen presents values of G that remain always lower than the virgin ones, the N02 nanomodified specimen instead shows a value of critical energy release ratio G_C (in correspondence of the first force peak, when the damage propagation starts) significantly lower than the same quantity evaluated for virgin specimens, but at the same time the curve monotonically rises with the crack length and the fracture toughness during the propagation phase keeps on increasing, until it oversteps the virgin values approximately when the crack length reaches 100 mm. This means that, restricting to the N02 nanomodified specimen, although the nanomat seems to worsen the damage initiation conditions of the bonded joint, the steady-state value of fracture toughness G_{ss} is greater, resulting in a bigger amount of the damage dissipated energy with respect to the virgin one: initially the presence of the nanomat in the interface encourages the damage

initiation, but suddenly the crack is obstructed by the nanofiber, making the damage path dissipate more energy to propagate. This could be probably due to the nanomat capability, already observed in the interfaces of composite laminates, to enable a 'bridging effect' through the opposite sides of the bonding interface. Therefore, the tendency of the nanomat to behave like a net-like reinforcing web, exhibited if used in combination with composite materials, seems to be confirmed also when using the nanomat like an adhesive carrier, even if limited only for one of the two tested specimens with nanofiber.

4. Conclusions

In the present paper, the use of an electrospun nanofiber mat as adhesive carrier in bonding joints was evaluated. An experimental campaign was performed by means of the manufacturing of 2024-T3 aluminum alloys bonded with an epoxy impregnation resin for woven pre-pregs and the subsequent comparison between simple bonded joints and joints with a Nylon 6,6 nanofiber mat interleaved in the interface and impregnated by the epoxy resin. A 40 mm thick crack was artificially induced through the insertion of a polyester sheet. Some 60 μm thick metal sheets were used to calibrate the thickness of the interface and to make it uniform in both the virgin and the nanomodified specimens. The curing cycle was performed under vacuum in order to increase the air ejection from the adhesive. Two specimens for each configuration (virgin and nanomodified) were tested. The results of the DCB tests were diversified. The first nanomodified specimen exhibited a trend of the Mode I fracture toughness which remained always lower than the virgin ones. The second nanomodified specimen instead presented a value of critical fracture toughness G_C significantly lower than the virgin one, but on the other hand the fracture toughness kept on increasing monotonically, until it reached the peak of 0.25 N/mm when the crack length was approximately 124 mm, exceeding by far the corresponding virgin values for the same crack length. This could mean that the presence of the nanomat does not succeed to tough the interface with respect to the damage initiation, but it can raise the amount of damage dissipated energy, slowing down the crack propagation and the catastrophic breakage. This properties could be used to make the nanomat being successfully used to act as an adhesive carrier in those applications in which an increase of the dissipated energy is involved and it is more desired than an high strength of the bonding to the damage initiation. Future development of the works will be represented by further tests to validate the trend shown by the second nanomodified specimen, combined with microscopic and SEM analysis to better examine the fracture surface and to understand the reason why the two nanomodified specimens show a mismatching behavior during the crack propagation phase. Other tests will be performed for both investigating the effects leading by the nanomat to other failure modes and evaluating the properties of the adhesive and the influence that the mechanical parameters has over the bonding toughening with nanofiber mats.

References

da Silva, L. F. M., Ochsner, A., and Adams, R. D., Handbook of Adhesion, Technology, (Springer, Berlin, 2011).

Giuliese, G., Palazzetti, R., Moroni, F., Zucchelli, A., Pirondi, A., Minak, G., Ramakrishna, S. 2013. Experimental and numerical study of the effect of Nylon 6,6 electrospun nanofibrous mats on the delamination of CFR-epoxy composite laminates. 19th International Conference on Composite Materials.

Huang, Z. M., Zhang, Y. Z., Kotaki, M., and Ramakrishna, S., Compos. Sci. Technol. 63, 2223–2253 (2003).

Krenk, S. 1992. Energy release rate of symmetric adhesive joints. Engineering Fracture Mechanics, vol. 43, pp. 549-559.

Musiari, F., Giuliese, G., Pirondi, A., Zucchelli, A. 2015. Development of a workflow for the virtual optimization of a nanofiber-interleaved composite laminate subjected to impact loading. 20th International Conference on Composite Materials.

Oh, H. J., Kim, H. Y., Kim, S.S. (2014) Effect of the Core/ Shell-Structured Meta-Aramid/Epoxy Nanofiber on the Mechanical and Thermal Properties in Epoxy Adhesive Composites by Electrospinning, The Journal of Adhesion, 90:9, 787-801.

Palazzetti, R., Zucchelli, A., Trendafilova, I. 2013. The self-reinforcing effect of Nylon 6,6 nano-fibres on CFRP laminates subjected to low velocity impact. Composite Structures, vol. 106, pp. 661-671.

Zucchelli, A., Focarete, M.L., Gualandi, C., Ramakrishna, S. Electrospun nanofibres for enhancing structural performance of composite materials. Polym Adv Technol 2011;22(3):339–49.